

THIN-FILM INTRACORTICAL RECORDING MICROELECTRODES

Quarterly Report #6

(Contract NIH-NINDS-NO1-NS-7-2364)

July - September 1998

Submitted to the

Neural Prosthesis Program

National Institute of Neurological Disorders and Stroke
National Institutes of Health

by the

Center for Integrated Sensors and Circuits

Department of Electrical Engineering and Computer Science
University of Michigan
Ann Arbor, Michigan
48109-2122

October 1998

Summary

This contract calls for the development of active probes for neural recording. A 64-site 8-channel probe with site selection and signal buffering but no multiplexing is in development as is a high-end multiplexed version of this device that includes gain. During the past quarter, work concentrated in several areas: 1) we have successfully used the active probes to record multiple single units from the cerebellar cortex of an experimental animal. The data were multiplexed on the chip to a single data line and demultiplexed off chip and passed to our data acquisition equipment in the usual manner as with passive probes. 2) We have completed the design of an improved input circuitry for use with an integrated wireless version of the probe electronics; and 3) We have conducted experiments with passive probes designed to help us understand the recording characteristics of different sized sites. Work in these areas is discussed in the following sections.

Thin-Film Intracortical Recording Microelectrodes

1. Introduction

The goal of this program is the realization of batch-fabricated recording electrode arrays capable of accurately sampling single-unit neural activity throughout of volume of cortical tissue on a chronic basis. Such arrays will constitute an important advance in instrumentation for the study of information processing in neural structures and should also be valuable for a number of next-generation closed-loop neural prostheses, where stimuli must be conditioned on the response of the physiological system.

The approach taken in this research involves the use of solid-state process technology to realize probes in which a precisely-etched silicon substrate supports an array of thin-film conductors insulated above and below by deposited dielectrics. Openings in the dielectrics produced using photolithography form recording sites, which permit recording from single neurons on a highly selective basis. The fabrication processes for both passive and active (containing signal processing circuitry) probe structures have been reported in the past along with scaling limits and the results of numerous acute experiments using passive probes in animals. In moving to chronic implant applications, the major problems are associated with the probe output leads, both in terms of their number and their encapsulation. The probe must float in the tissue with minimal tethering forces, limiting the number of leads to a few at most. The encapsulation of these leads must offer adequate protection for the megaohm impedance levels of the sites while maintaining lead flexibility.

Our solution to this problem has involved two steps. The first has been to embed circuitry in the probe substrate to amplify and buffer the signals and to multiplex them onto a common output line. Using this approach, signal levels are increased by factors of about 300, impedance levels are reduced by four orders of magnitude, and the probe requires only three leads for operation, independent of the number of recording sites. A high-yield merged process permitting the integration of CMOS circuitry on the probe has been developed, and this circuitry has been designed and characterized. The second step has involved the development of silicon-based ribbon cables, realized using the same probe technology, to conduct the neural signals to the outside world. These cables have shown significant advantages over discrete leads, both in terms of the ease with which chronic implants can be assembled and in terms of the ability of the cables to survive long-term biased soaks in saline. The cables can be built directly into the probes so that they come off of the wafer as a single unit, requiring no joining or bonding operations between them. The cables are significantly more flexible than were previously used discrete wire interconnects.

This contract calls for the development of active probes for neural recording. A 64-site 8-channel probe with site selection and signal buffering but no multiplexing is in development as is a high-end multiplexed version of this device that includes gain. During the past quarter, work concentrated in several areas: 1) we have successfully used the active probes to record multiple single units from the cerebellar cortex of an experimental animal. The data were multiplexed on the chip to a single data line and

demultiplexed off chip and passed to our data acquisition equipment in the usual manner as with passive probes. 2) We have completed the design of an improved input circuitry for use with an integrated wireless version of the probe electronics; and 3) We have conducted experiments with passive probes designed to help us understand the recording characteristics of different sized sites. Work in these areas is discussed in the following sections.

2. Passive Probe Developments

The distribution of passive probes to external investigators continues through the Center for Neural Communication Technology. In conjunction with this activity, two new mask sets were designed and began fabrication during the last quarter. The "STANDARDS" mask set includes 27 probe designs that will comprise the new passive probe catalog. These designs were chosen based on input from our external users and include designs intended for both acute and chronic use. The bond pads have been standardized to permit easier integration with a variety of assemblies, such as the one being developed by Bioelectric Corp. in Portland, OR. The different designs vary in shank length, site spacing and number of shanks. There are also several designs with sites configured as tetrodes.

The "CNCT4" mask set includes 22 designs submitted by both internal and external collaborators. Investigators with custom designs on this set include Drs. William Agnew and Douglas McCreery of the Huntington Medical Research Institutes, Dr. David Edell of MIT Lincoln Labs, Dr. Gyorgy Buzsaki of Rutgers University, Dr. James Weiland of Johns Hopkins University, Dr. Wayne Cascio of UNC Chapel Hill, and Dr. John Middlebrooks of the University of Michigan. Several new "brain-in-the-box" designs (see Quarterly Report #5) with 32 channel capability are also included. The mask sets are being processed in parallel and should be through fabrication by the end of the next quarter.

3. Active Three-Dimensional Recording Probe Arrays

In order to instrument a large population of neurons simultaneously and to achieve high-quality neural recordings, advanced microelectrode arrays with on-chip signal processing circuitry are critically needed. Such active probes would lower the output impedance of the recording channels, improve the signal-to-noise ratio, reduce the number of the interconnection leads, and ease the encapsulation requirement of the recording systems. At Michigan, we have made great effort on the development of active probe technologies, and made significant progress in the design, fabrication, and testing of active 2D and 3D probe arrays.

A set of active recording probes have been designed and fabricated recently in which each probe design tests a certain basic circuit function, including buffering, amplification, and multiplexing. The evaluations of these circuit blocks in terms of power, area, noise, and gain, and the detailed study of issues such as dc baseline stability, multiplexer clock noise, and the role of the bias applied to the probe substrate, is setting the stage for the circuit blocks to be used in higher-level probes to be integrated later this

year. As reported previously, we have now been testing these active probes extensively, and have presented successful in-vivo recordings using some of the probe designs.

We have demonstrated three different types of buffered probes, namely "BUF1", "BUF2", and "BUF3", fully functional. The in-vivo recordings with pairs of active and passive sites 15 μm apart on these buffered probes have shown that on-chip signal processing is possible without compromising signal-to-noise ratios. In-vitro data analysis has shown that both active and passive recording channels have background noise level of around 7 μV -rms. We have demonstrated low noise recording capability with the multiplexed probes. These probes have four recording channels buffered and then multiplexed into one data output line at a sampling rate of 240 kHz. The clock used for sampling is generated externally, which is low duty-cycle in order to avoid transition glitches at the middle of the sampling window. The on-chip multiplexing and off-chip demultiplexing system typically has a noise level of 14 μV -rms in vitro, compared to 9 μV -rms noise level of the system when the sampling clock is disabled (just buffering, no multiplexing). The background noise of the whole system can be further reduced if some gain can be provided at front-end before multiplexing. We also have several amplifier probes designed and tested, and in-vivo recordings have been obtained with these probes. Table 1 summarizes some of the parameters measured from the amplifier probes.

Among the four amplifier designs, only "AMP3" is closed-loop, whose schematic is shown in Fig. 1. A closed-loop amplifier is highly desirable because the voltage gain is set by the feedback loop, which is typically composed of resistors and less sensitive to the process parameters. Not like the "AMP2" and "AMP4" that have internal band limiting (dc feedback) to suppress dc offsets at the recording input, "AMP2" has an input diode as a loading device to attenuate the dc offset seen by the operational amplifier. The dc offsets at the recording sites referring to the ground reference electrode exist because of the open-circuit potential of the electrode material drifting randomly and/or the potential difference between the two electrodes made of different materials. Without internal band-limiting, certain type of input loading device has to be provided to prevent the high-gain amplifier from saturation, as shown in Fig. 2. Periodically discharging the recording site at very frequency rate using a pair of reset gates is an option, but it needs very low-frequency control signal/clock which may need large area to implement or need an extra output leads. An input resistor is actually an ideal candidate, and according to the impedance-frequency characteristics and the dc characteristics of the iridium electrodes (Figs. 3 and 4), having resistance between 60 M Ω and 1 G Ω should be sufficient to suppress the dc offset without compromising the ac signal. However, it is impractical to implement such a high-resistance resistor on-chip due to the very large area it requires. On the other hand, a zero-biased diode theoretically should have resistive characteristics, and it is easy to achieve high resistance in small area. Therefore, a simple input-clamping diode having an area of 800 μm^2 is chosen as a dc-baseline stabilization scheme in the "AMP3" design.

However, as reported previously, the initial experiments with probes "AMP3" in vitro and in vivo show an unstable performance of the amplifier, which sometimes worked normally, but got saturated many other times. So we started to investigate the dc characteristics of the iridium electrodes and the I-V characteristics of the input diode. According to Figs. 3 and 4, a leakage current of 1 pA or more at the pn junction of the

diode should be sufficient to polarize the $100\ \mu\text{m}^2$ Ir recording electrode and stabilize the dc baseline. But we have found that, due to the photogenerated current and other parasitic effects, the I-V curve of the input diode usually does not cross the origin as shown in Fig. 5. On the other word, the voltage offset of the diode itself can reach hundreds of millivolts and saturate the amplifier.

To verify the above cause for the saturation of the amplifier and make the probe "AMP3" working more stable in vitro or in vivo, the circuit routing was modified so that the input-clamping diodes and the feedback resistors of all four channel were connected together and biased externally as shown in Fig. 6. By adjusting the bias voltage, we have been able to polarizing the recording sites to such a level that the voltage drop across the diodes is close to zero and the amplifiers are therefore in the working range. Figure 7 is the frequency response of the "AMP3" in vitro, which has a gain close to 40 dB, a higher cutoff frequency of 13 kHz, and a lower cutoff frequency less than 10 Hz (not showing in the figure). In the dark, the bias voltage was typically within plus/minus tens of millivolts range; while with normal room lighting, the bias was usually hundreds of millivolts below zero. This makes sense because the light generates positive current across the n-p junction and polarize the recording electrode in the negative direction.

Using the same method, we have been able to record single-unit responses from both guinea pig cerebellum and cochlear nucleus as shown in Figs. 8 and 9. It needs to mention that all four channels could not be tuned in at the same time (three channels at most) in the tissue, though there was no problem to tune in all the channels simultaneously in buffered saline. The situation also changed at different locations in the tissue. This was perhaps because of the inhomogeneous nature of the tissue and thus different polarization current were required for different channels, depending on the locations of the electrodes.

To make the closed-loop amplifier "AMP3" working more stable and less sensitive to the light and other parasitic effect, other schemes need to be explored. In fact, a subthreshold-biased PMOS transistor should be able to serve the purpose. We have measured some of the MOS transistors on the wafers of active probes, and the I-V characteristics of a PMOS transistor with w/l ratio of 20/15 is shown in Fig. 10. Biased at 60 mV below the threshold voltage, this transistor has excellent resistive characteristics near the zero region of V_{ds} , having a resistance of $20\ \text{M}\Omega$. This implies that a resistance around $60\ \text{M}\Omega$ to $1\ \text{G}\Omega$ is achievable. It is felt that the higher the resistance, the more susceptible the load device is to the parasitic effects. Thus, it should be very cautious to use a resistance higher than $1\ \text{G}\Omega$, and preferably to have a resistance of $500\ \text{M}\Omega$ or less (2 pA or more polarization current).

Since we have characterized different designs of voltage buffering, amplification, and multiplexing, and demonstrated successful in-vivo recording capability using the active probes with acceptable noise level, we are ready to put all the function blocks together and design large active recording probe systems with addition functions such as site activation, site impedance testing, electrode continuity checking, etc.

Probe Type	AMP 1	AMP 2	AMP 3	AMP 4
Amplifier Type	open- loop	open- loop	close d-loop	open- loop
Input Stabilization	Ir reference	dc feedback	input diode	dc feedback
Layout Area (mm ²)	0.051	0.112	0.083	0.105
Voltage Gain (dB)	42	25	40	36
Bandwidth (Hz)	3k	35 - 30k	10 - 13k	400 - 12k

Table 1: Measured performance of the front-end amplifiers.

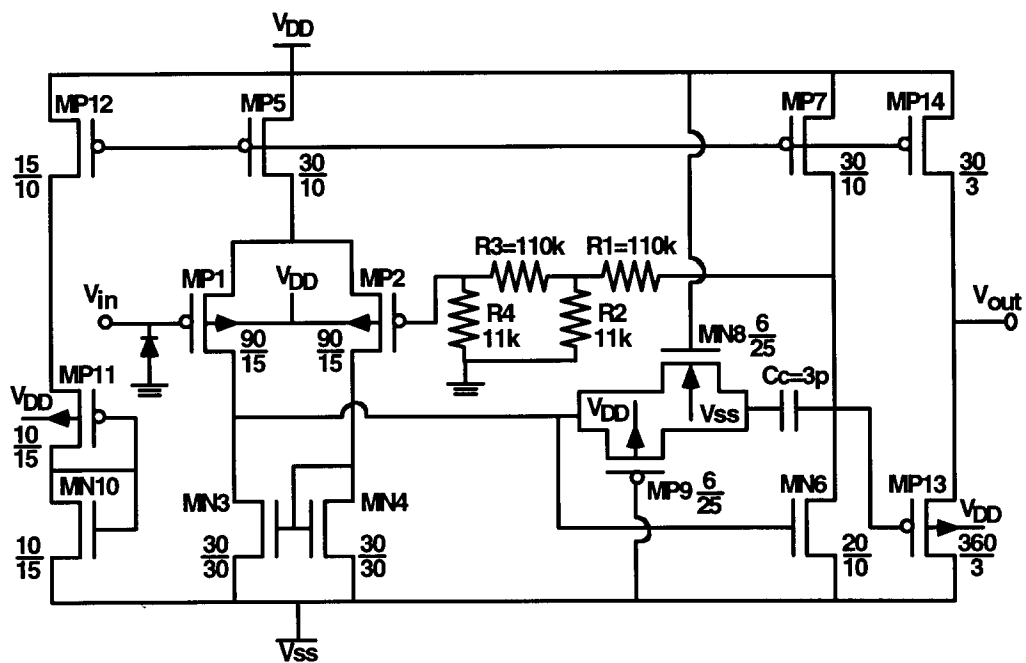


Figure 1: The schematic of the closed-loop amplifier "AMP3" with an input diode for dc-baseline stabilization.

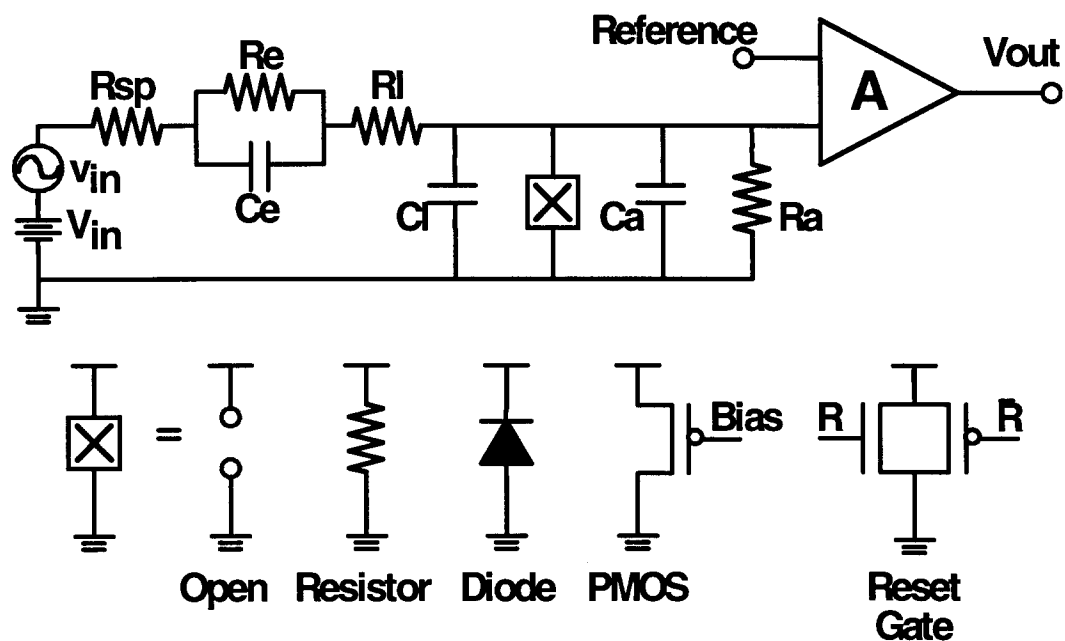
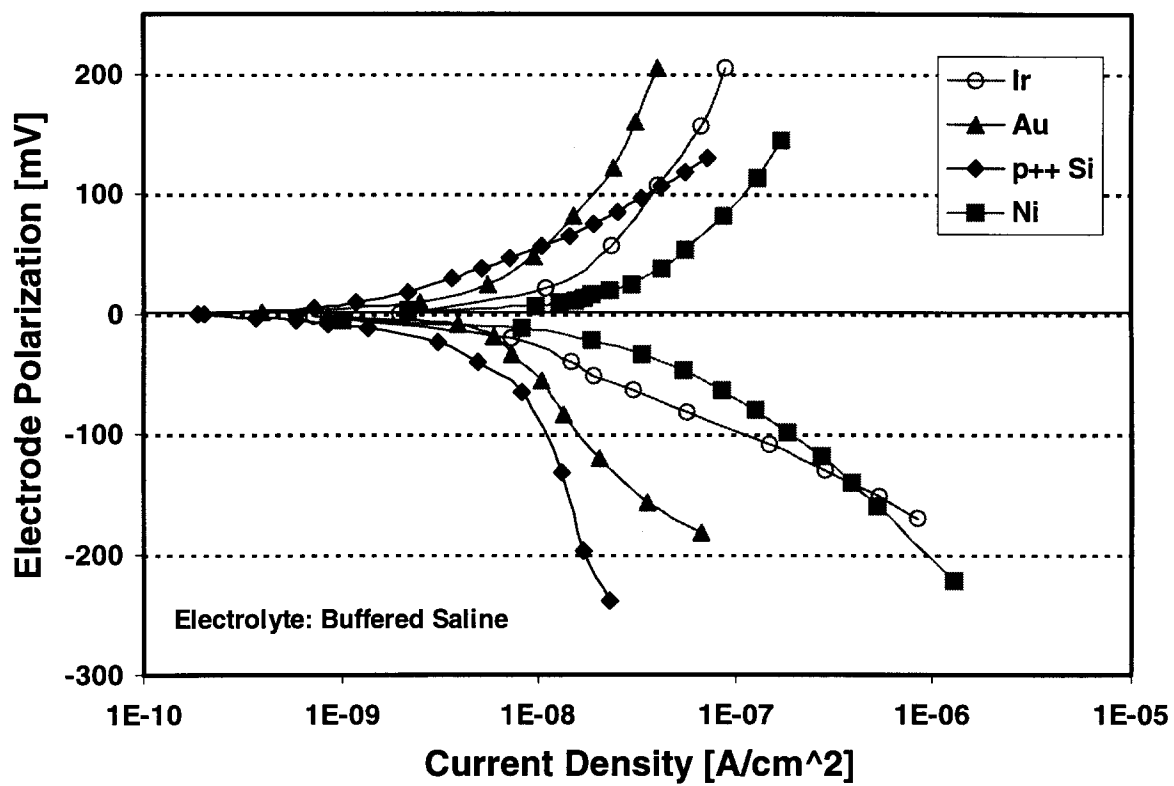
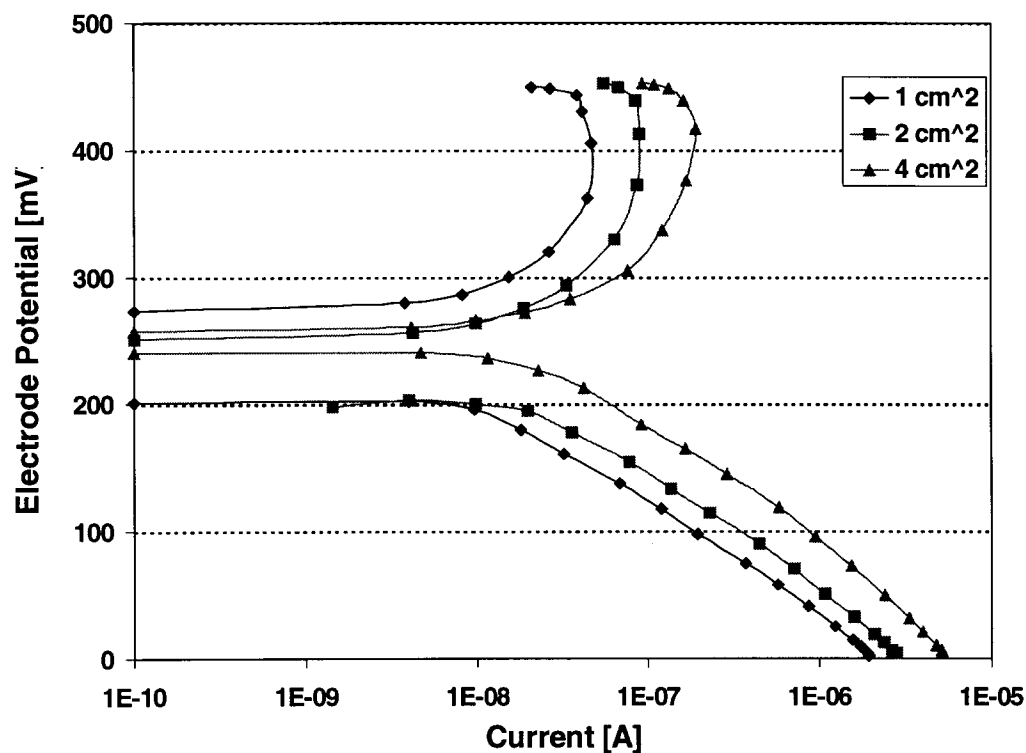


Figure 2: An equivalent circuit model of electrode-electrolyte-amplifier interface and associated input loading devices for dc-baseline stabilization.



DC Characteristics of Thin-Film Electrodes

Figure 3: DC characteristics of thin-film electrodes.



DC Characteristics of Iridium Electrodes with Different Areas

Figure 4: DC characteristics of iridium electrodes in buffered saline with different areas.

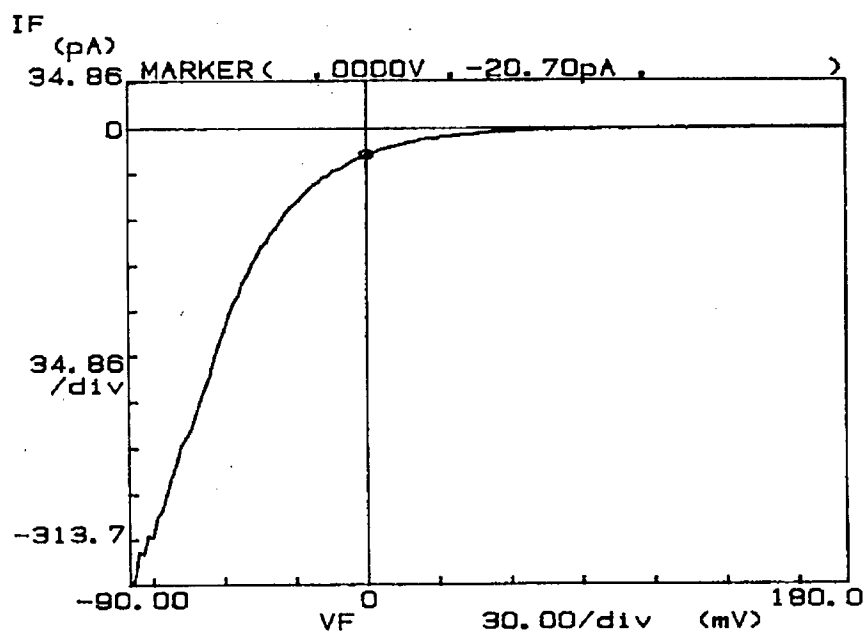


Figure 5: I-V characteristics of the input diode used in probe "AMP3" with normal room lighting.

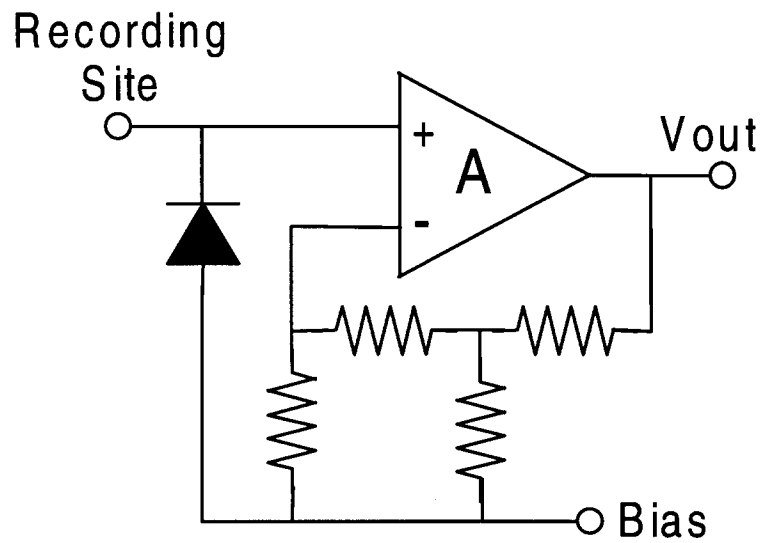


Figure 6: The schematic of the "AMP3" with its input diode and feedback resistor biased externally.

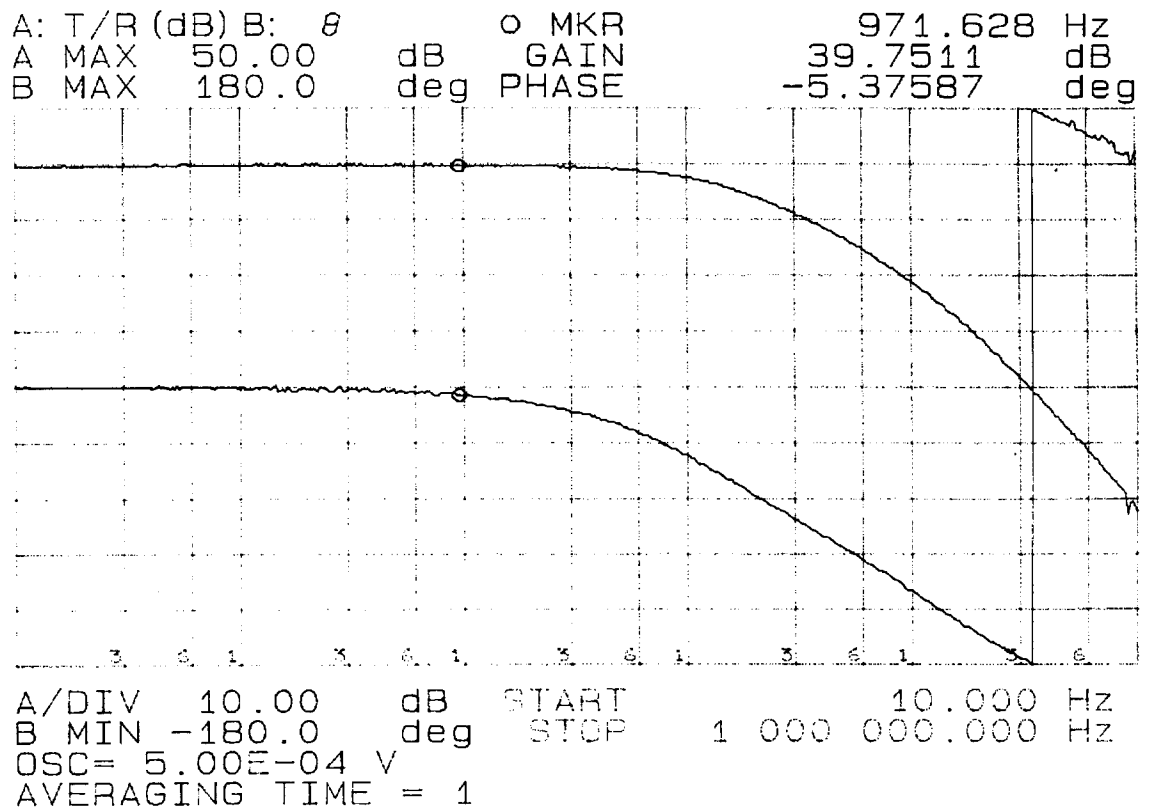


Figure 7: Frequency response of the "AMP3" in vitro.

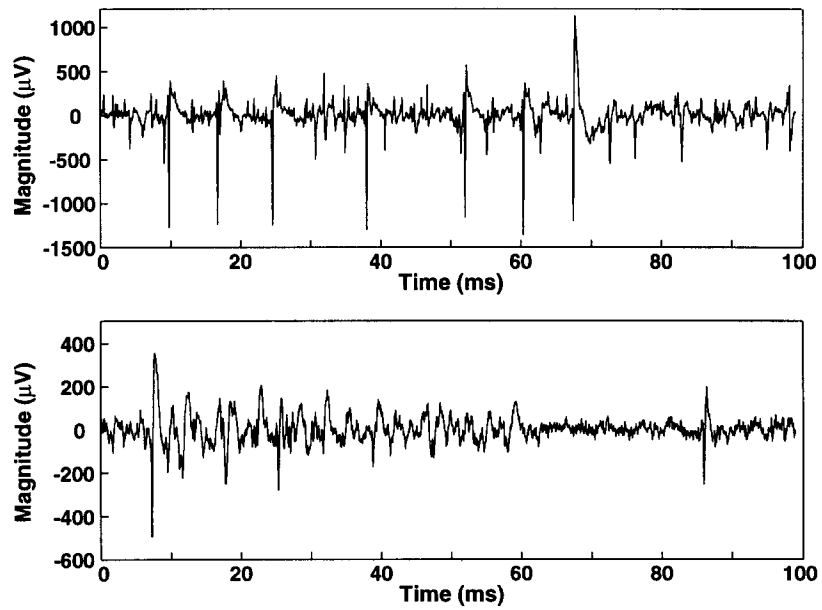


Figure 8: Neural recordings obtained with probe "Amp3": spontaneous activity in guinea pig cerebellum (top) and neural response driven by white noise bursts in cochlear nucleus.

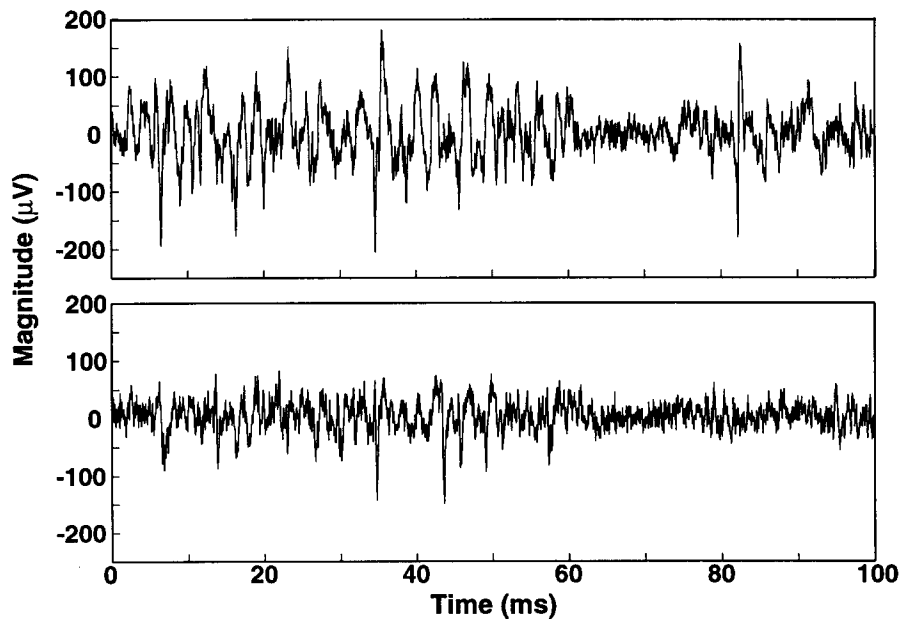


Figure 9: Simultaneous neural responses driven by noise bursts recorded with probe "AMP3".

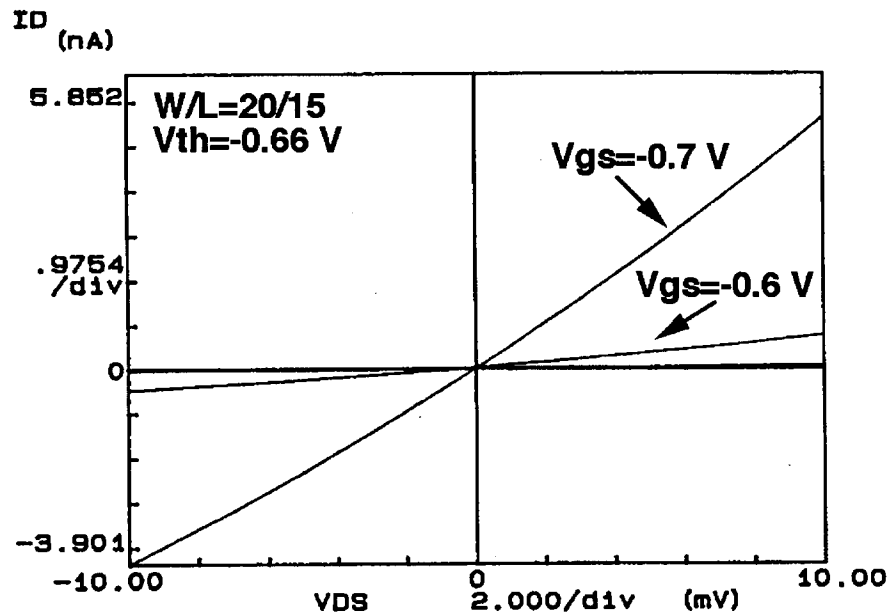


Figure 10: I-V characteristics of a subthreshold-biased PMOS transistor with a w/l ratio of 20/15.

4. Use of Parylene Ablation for Post-Processing Site Formation

In previous quarterly reports we reported on the use of Parylene to define site shape/size of larger SX04 (4000 μm^2) electrode sites. In the last quarterly report we showed recordings taken from one of these re-opened (ablated) electrodes. This quarter we moved the electrode past a cerebellar neuron passing it from site to site. Figure 1 shows the peak to peak amplitude of the neuron as it was passed from site to site. Channels 1 and 5 are 10x10 μm and are at the tip of the electrode. Sites 2 and 4 are 15x15 μm and are the next two electrodes from the tip. Site 3 is 20x20 μm and is the top site. The 15x15 μm and the 20x20 μm sites recorded a much larger peak to peak voltage than the 10x10 μm sites. Figure 2 shows the RMS voltage by depth for each of the electrode sites. The 15x15 μm and the 20x20 μm sites initially have a lower RMS noise level, but increases as the site moves into the area of the neuron. In the next quarter we plan to repeat these experiments to see if this trend is what can be expected from recording electrodes of these sizes. In the future we would like to try other sized sites to determine if there is an optimal site size for recording cerebellar neurons, which may be different than for neurons in other areas of the brain.

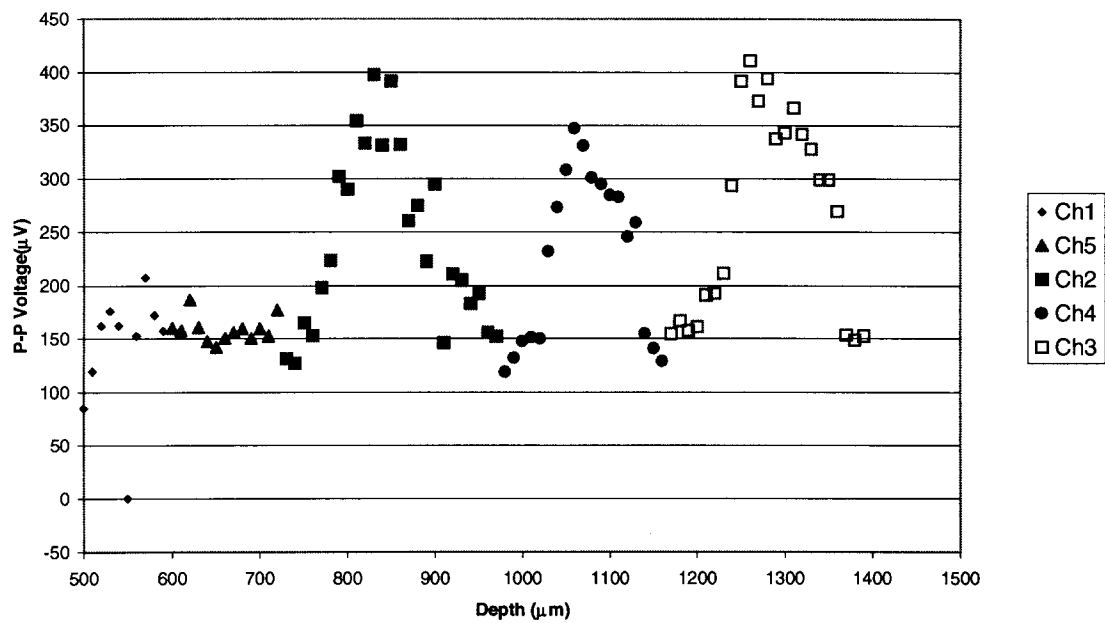


Figure 11: Probes with different site sizes are passed by a cell in the cerebellum. The larger sites measure a larger potential from the cell at closest approach while the smaller sites have smaller potentials.

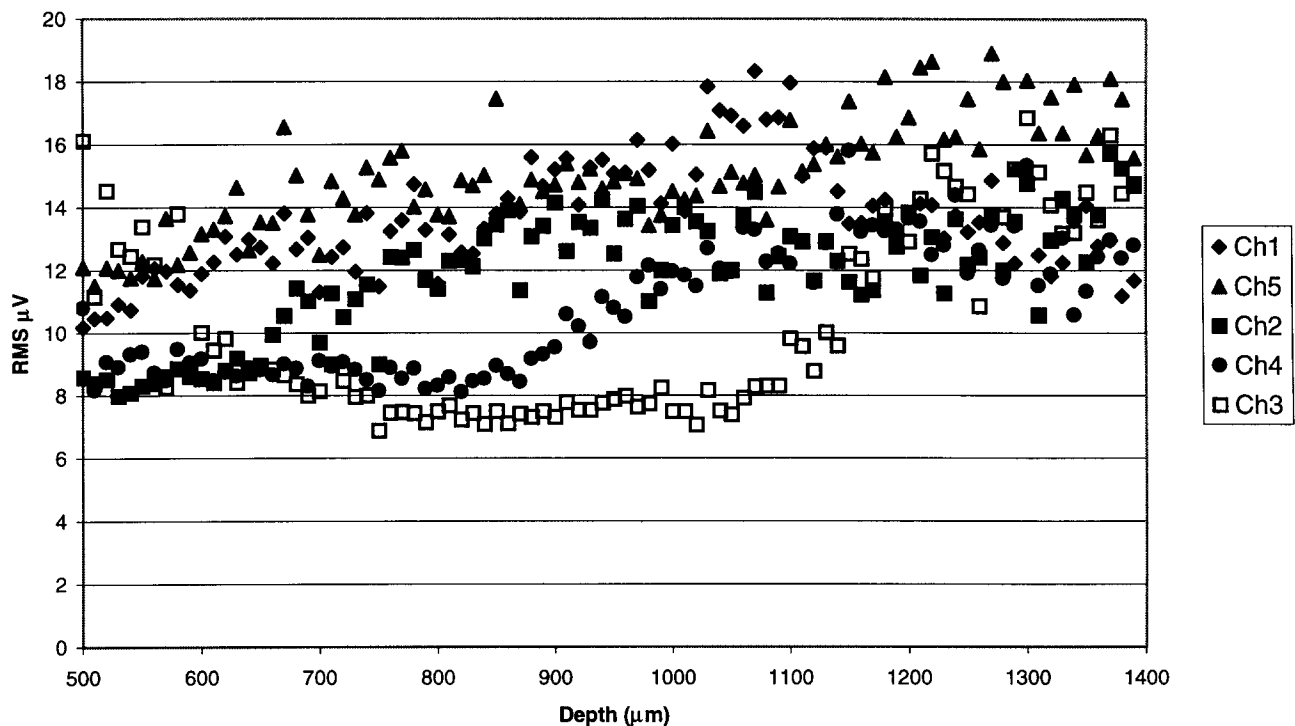


Figure 12: The noise characteristics of the same sites as in figure 11 are indicated above. The smaller sites tend to be more noisy both in active tissue containing cells and passive tissue which does not have recordable cells.

5. DC amplifier with feedback

Over the last quarter, we have accomplished the following goals in our research endeavors.

- Completion of the simulations of the new DC stabilization scheme (outlined in Quarterly Report #4 and #5).
- Layout of the DC stabilization circuit and DC feedback amplifier.

The block diagram for the new DC stabilization scheme has been shown below. Earlier Quarterly reports (#4 and #5) showed the preliminary simulation results, which demonstrated that the idea of actively clamping the DC offset (associated with the recorded neural signal) using an active device biased into the sub-threshold region is feasible. As mentioned earlier, the above system makes use of a transistor biased into the sub-threshold regime for synthesizing a high resistance "R_{ds}". The value of R_{ds} is critical to the operation of the system because it sets the low frequency cut off of the circuit. In fact, even though a DC feedback amplifier is connected to the front-end stage, the overall low frequency performance of the composite system is set by the front-end stage and not the amplifier. Thus, it was desired that the front-end circuit be made as robust as possible to any variations in

- Process Parameters

- Noise voltages
- Supply Voltage Drifts

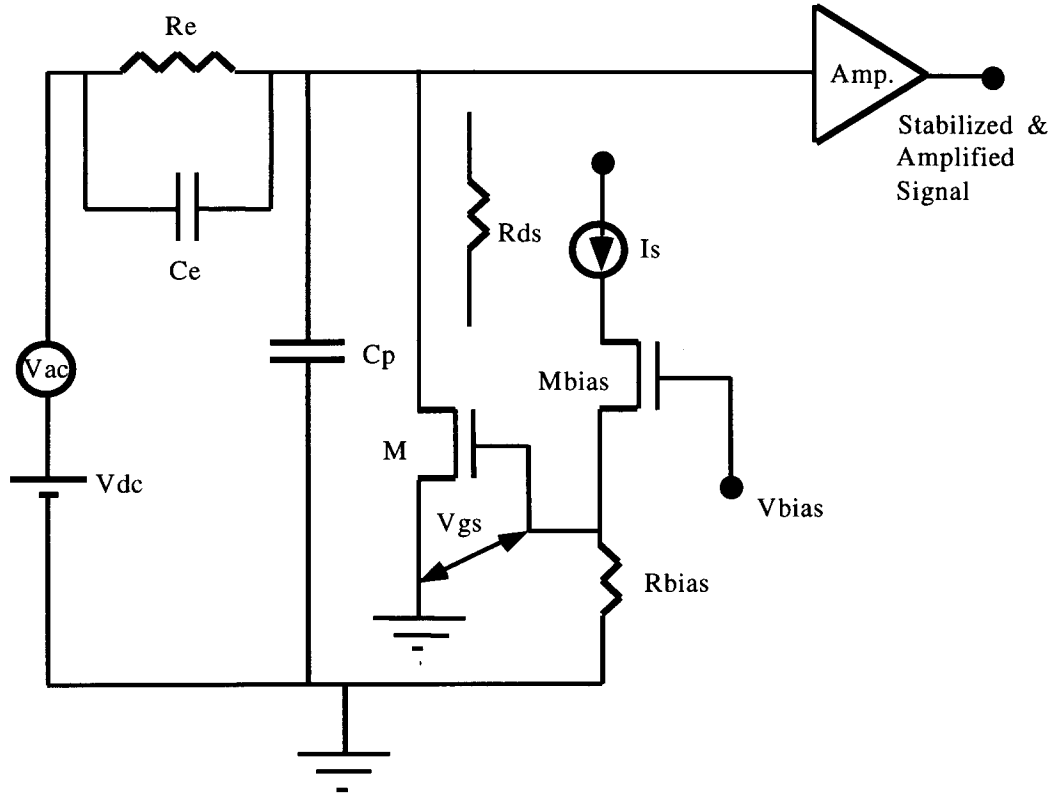


Figure 13: DC stabilization circuit

A number of simulations were done in HSPICE in order to remove circuit dependencies on the above effects.

Table 1. Shows the extent to which the designed circuit is stable to variations in process parameters, noise drifts, and supply voltage drifts.

PARAMETER TESTED	STABILITY
PROCESS PARAMETERS	15 %
NOISE DRIFT	25 %
SUPPLY VOLTAGE DRIFT	30 %

Table 2. Stability of the system to drifts in process parameters, noise and supply voltage

AC Response of the composite system:

Figure 14 shows the ac response of the DC Stabilization-Amplifier system. It may be noted that the plot has 3 curves. These represent the ac response of

1. Sub-threshold front end stage.
2. DC feedback amplifier.
3. Composite system.

It can be seen that both the front-end stage, as well as the amplifier have a frequency shaped gain variation. This was done so that any residual dc drift that is not attenuated by the front-end stage may be clamped by the amplifier. The overall gain of the system is merely the sum of the gains (in dB) of the individual stages. This composite gain varies from - 60 dB at dc to as high as + 55 dB in the mid-band (100 Hz to 10 k Hz). This is indicated in Fig 14 below.

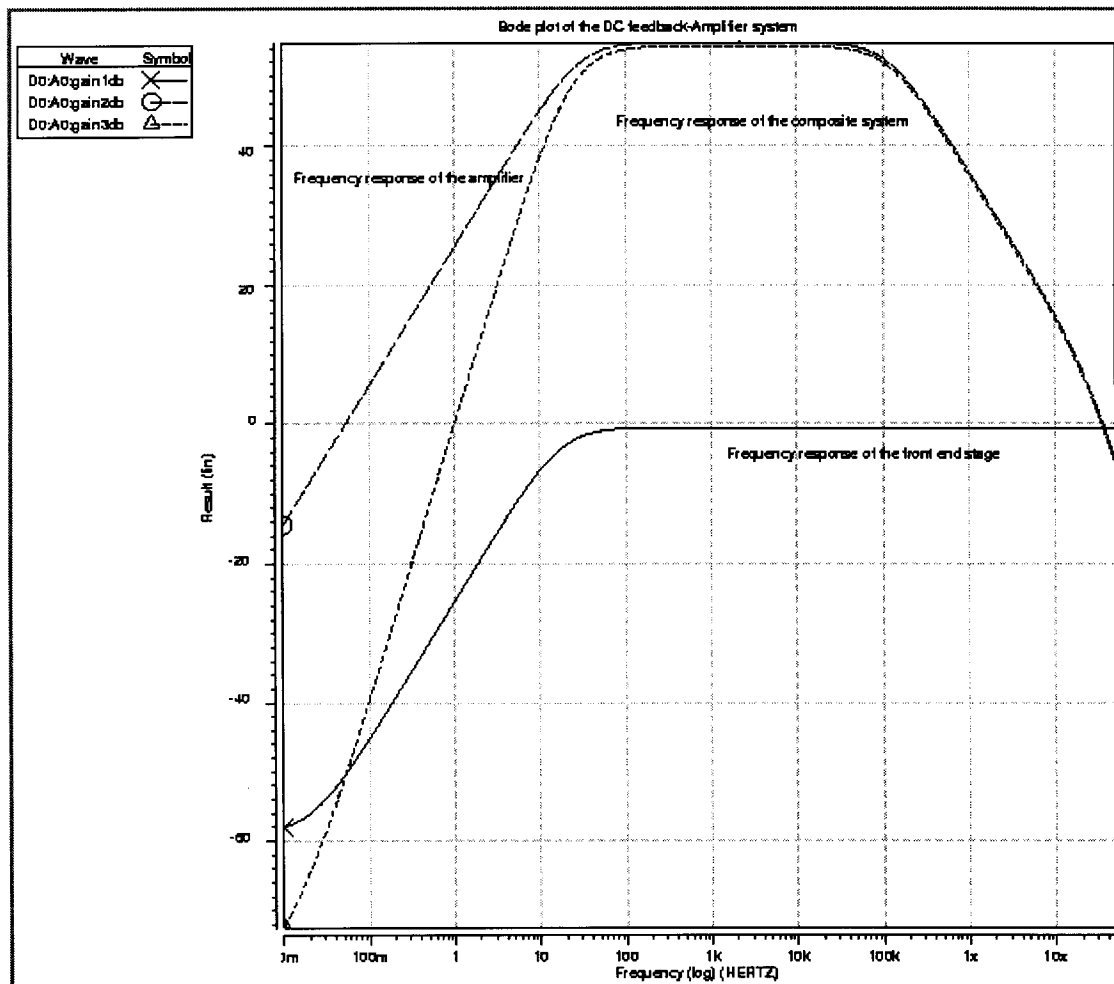


Figure 14: Bode plot of the DC Stabilization-Amplifier system

The above system is being laid out using a MOSIS-based AMI 1.2-micron process. In order to achieve a diode-capacitor low-pass filter, the analog NPN option of the MOSIS process is being utilized.

In conclusion, a new DC stabilization -DC feedback amplifier system has been developed. This system is capable of providing an attenuation of -60 dB in the stop-band and a gain of 55 dB in the pass band. The amplifier is of the open-loop type with DC feedback being realized with a diode capacitor arrangement.

The amplifier itself has the following specifications

- Type: 3-stage Operational Amplifier, Open-Loop, DC Feedback.
- Mid-Band Gain: 55 dB
- Unity Gain Frequency: 12.5 M Hz.
- Power Dissipation: 0.56 m W
- Unity Gain Phase Margin: 35 degrees

It is believed that if the above circuit is successfully fabricated, a major bottleneck facing the design of on-chip circuitry will have been removed and this will enable researchers to pursue more aggressive circuit designs.

Plan of action for the coming quarter:

The following activities have been planned for the forthcoming quarterly period.

- Completion of the layout of the above system and submission to the MOSIS service.
- Initiation of the circuit design for the wireless telemetry interface.